

## Review

# Nanostructures from alkyl vitamin C derivatives ( $ASC_n$ ): Properties and potential platform for drug delivery

Santiago Palma <sup>a</sup>, Ruben Manzo <sup>a</sup>, Pierandrea Lo Nostro <sup>b</sup>, Daniel Allemandi <sup>a,\*</sup>

<sup>a</sup> Departamento de Farmacia, Fac. de Ciencias Químicas, Universidad Nacional de Córdoba, Ciudad Universitaria, 5000 Córdoba, Argentina

<sup>b</sup> Dipartimento di Chimica, Università di Firenze, Via della Lastruccia 3, 50019 Sesto Fiorentino, Italy

Received 11 June 2007; received in revised form 11 September 2007; accepted 11 September 2007

Available online 19 September 2007

## Abstract

Alkyl vitamin C derivatives ( $ASC_n$ ) combine in their structure a lipophilic and a hydrophilic moiety and exhibit properties of typical surfactant molecules. Self-assembly properties of  $ASC_n$  depend on the length of *n*-alkyl fatty chain.  $ASC_n$  start to aggregate at temperatures (CMT, Krafft point) in which the solubility reaches the critical micellar concentration (CMC). Above this temperature,  $ASC_n$  can aggregate in micelles or gel phase, depending of alkyl side chain. Upon cooling, for less soluble derivatives ( $ASC_{12}$ ,  $ASC_{14}$  and  $ASC_{16}$ ) liquid-crystal structures named coagels are obtained. They are able to solubilized insoluble and unstable drugs, protect them from any possible aggressive environment and promote their permeation through skin. Besides, the rheological properties of the coagels would be adequate for topical administration of pharmaceutical. These systems possess very interesting properties making  $ASC_n$  coagels promising pharmaceutical platforms for drug delivery. Results from investigations about all these properties are described and analyzed. Also, the perspectives of these systems as drug delivery systems are discussed.

© 2007 Elsevier B.V. All rights reserved.

**Keywords:** Vitamin C; Coagel; Nanostructures; Drug delivery

## Contents

1. Introduction .....	26
2. Physical-chemical and self-assembly properties .....	27
2.1. Characteristics of $ASC_n$ .....	27
2.2. Phase behavior and aggregation properties .....	28
3. Aggregates and nanostructures as drug delivery systems .....	31
3.1. Drug load capacity .....	31
3.2. Rheology of nanostructured aggregates .....	33
3.3. "In vitro" permeation of $ASC_n$ and influence in drug absorption (enhancement properties) .....	33
4. Summary and perspective .....	34
Acknowledgements .....	34
References .....	34

## 1. Introduction

The production of nanostructures with specific properties is one of the most important fields for several applications, spanning from pharmaceutics to electronics, from material science to environment protection, and so forth.

Besides the characteristic features related to the size of nanoparticles, other specific physico-chemical properties are involved in the design, synthesis and use of new "smart" materials. For this reason, innovative chemicals with peculiar redox, thermal, pH, photochemical and chemical properties are of great interest as starting building blocks for higher hierarchy architectures.

Active pharmaceutic species usually carry specific chemical moieties that characterize their nature, chemical behavior,

\* Corresponding author. Tel.: +54 351 4334163; fax: +54 351 4334127.  
E-mail address: [dalemandi@fcq.unc.edu.ar](mailto:dalemandi@fcq.unc.edu.ar) (D. Allemandi).

and biological effects. Among these, extended (conjugated) unsaturated bonds, large hydrophobic regions, polar groups with pH-responsive properties, and acceptor/donor residues for hydrogen or coordination bonding are the most important and often lead to the formation of supramolecular self-assemblies in water.

However, the activity and storage of these materials are often challenged by environmental conditions such as oxidative stress (mainly due to dissolved oxygen and its radical derivatives such as  $\cdot\text{OH}$  and  $\cdot\text{OOH}$ ) and pH if the dispersing medium.

L-Ascorbic acid (vitamin C, VC) is one of the best candidates for the protection of important, valuable, yet delicate species such as other vitamins (tocopherols), polyunsaturated molecules (carotenes, omega-3 and omega-6 acids), and other materials that are particularly sensitive to oxidation and in general to radical attack. The structural properties of VC meet some of these requirements. The presence of the  $\text{HO}-\text{C}=\text{C}-\text{OH}$  group in the lactone ring makes it an efficient reducing agent ( $E^\circ = +0.23$  V). On the other hand, the presence of several hydrophilic residues (hydroxyl groups and the lactone ring) as well as the chiral centers originates the rigid conformation of VC and the intermolecular interactions (hydrogen bonds) it can establish with the solvent and other molecules.

VC is readily oxidized to dehydroascorbic acid through a radical reaction, and therefore acts as an efficient, powerful, natural, and – above all – biocompatible and cheap antioxidant. However, its use is severely limited by its very poor solubility in almost all solvents, be they polar or apolar, with the exception of water (40% at 45 °C: Merck Index, 13th edition). This is the main reason why, for example, VC cannot penetrate across biomembranes, or is useless in the stabilization of small or large hydrophobic molecules. Therefore, the production of VS derivatives that are oil friendly and carry the desired antioxidant moiety is so welcome.

The antioxidant properties of L-ascorbic acid, or vitamin C (VC), are well known. This water soluble compound efficiently protects important organic and biological molecules against oxidative degradation. VC has been used in cosmetic and dermatological products since it has many favorable effects on the skin (Silva and Maia Campos, 2000). As a reducing agent, VC can scavenge and inhibit oxidizing agents and radicals. VC also improves the elasticity of the skin by promoting the formation of collagen (Djerassi, 1997).

Other limiting property related to the formulation of vitamin C is its very low chemical stability since under aerobic conditions it is oxidized (Kleszczewska, 2000).

In order to offer a wide selection of VC derivatives that comply with these requirements, amphiphilic derivatives seem to be the best choice. Single or double chain (Lo Nostro et al., 2007) surfactants, and bolaamphiphiles (Ambrosi et al., 2006) have been synthesized, and their phase behavior has been investigated. These surfactants are not only responsible for increasing the solubility of VC in hydrophobic media, but – through their self-association – they offer also an ideal environment for the stabilization of delicate lipophilic species in a protected (micellar) microcompartment. The most promising site for covalent bonding of a hydrophobic tail appears to be the primary OH

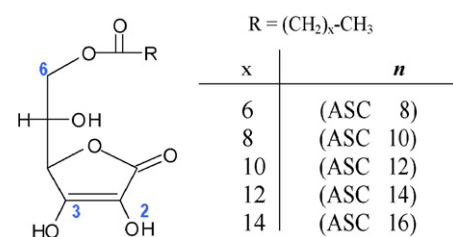


Fig. 1. Schematic chemical compositions of 6-*O*-alkyl ascorbic acid derivatives ( $\text{ASC}_n$ ).

group in position 6 that can easily form esters with high yields, while keeping the VC ring intact. Other derivatives can be synthesized, by using the OH groups in different positions (mainly 2 and 3), but the synthetic paths are usually much more complicated, they require more steps, and lead to significantly lower yields in the final product (Shibayama et al., 2005).

To overcome these two principal drawbacks, more lipophilic derivatives of VC were synthesized ( $\text{ASC}_n$ , Fig. 1). From this series, ascorbyl palmitate ( $\text{ASC}_{16}$ ) was the first synthesized derivative and has been shown to be as biologically active as its original hydrophilic counterpart.  $\text{ASC}_{16}$  is used either alone or in combination with alpha tocopherol as a stabilizer for oils in oral pharmaceutical formulations and food products (GRAS listed). Also, it can be used as an antioxidant in oral and topical preparations for drugs unstable to oxygen (Rowe et al., 2006).

Variations in alkyl chain length of the fatty acid also produce changes in the physical chemical properties of the derivatives. Consequently,  $\text{ASC}_n$  present the typical properties of surfactants such as potential solubilization of low solubility drugs and formation of different aggregates. These particular properties of  $\text{ASC}_n$  have not been explored for its potential useful in the pharmaceutical field.

The goal of this article is to describe research findings concerning with the properties of  $\text{ASC}_n$  and the supramolecular aggregates that these compounds can form. Also, some pharmaceutical relevant properties such as solubilization, stabilization and permeation enhancement of drugs are reported and analyzed.

## 2. Physical-chemical and self-assembly properties

### 2.1. Characteristics of $\text{ASC}_n$

As previously introduced,  $\text{ASC}_n$  are obtained through the esterification of hydroxyl group in position 6 of VC with fatty acids of variable length chain (Fig. 1). The acid strength of the derivatives remains similar to that of VC, with  $\text{p}K_a = 4.2$  for –OH group in position 3 and  $\text{p}K_a = 11.6$  for –OH group in position 2. Also the redox properties of VC are maintained in its amphiphilic 6-*O*-alkanoates, as shown by the instantaneous decoloration of  $\text{Br}_2$  in acetone, upon addition of a small amount of  $\text{ASC}_n$ , and by the antioxidant tests carried out on ethyl linoleate, whose peroxidation was started by a radical initiator (AIBN in hexane), and temporally stopped by the VC derivatives. The synthesis of  $\text{ASC}_n$  was reported elsewhere (Capuzzi et al., 1997). The variation in side chain length has a direct influence on their physico-chemical properties, for example the

Table 1

Melting point and TMC (°C) of  $ASC_n$  aqueous dispersions (from Palma et al., 2002a)

Compound	Melting point (°C)	DSC	Conductivity
$ASC_8$	87.0–88.0	18.5	19.3
$ASC_{10}$	96.0–98.0	34.5	36.8
$ASC_{12}$	105.5–106.5	47.3	44.5
$ASC_{14}$	108.0–109.0	56.0	54.2
$ASC_{16}$	113.0–114.0	63.8	61.3

melting point increases with the side chain length (see Table 1) (Palma, 2003). The derivatives with six or eight atoms of carbon have enough solubility at room temperature to form stable supramolecular aggregates in water (Lo Nostro et al., 2000a,b) while for  $n > 10$  it is necessary to raise the temperature until the solubility reaches the critical micellar concentration (CMC). This temperature dependence of surfactants' solubility indicates the existence of the so-called Krafft temperature or Krafft point (critical micellar temperature, CMT) (Clint, 1992; Myers, 1994). The CMT of  $ASC_n$  derivatives increases as the length of hydrocarbon chain becomes longer and, as can be expected, the kind of aggregates that can be formed above CMT is also dependent of the structure of derivative (Capuzzi et al., 1996a,b, 1997).

## 2.2. Phase behavior and aggregation properties

The phase behavior of  $ASC_n$  is probably the most interesting physico-chemical evidence of the complicated set of different intermolecular interactions (hydrophobic and electrostatic interactions, and hydrogen bonding), that control the thermal behavior of aqueous dispersions of these surfactants.

At temperatures higher than CMT,  $ASC_n$  form clear dispersions (Kohler et al., 1988). On cooling, water dispersions of ascorbyl-alkanoates form "coagels" regardless of the length of the aliphatic chain (Palma, 2003; Palma et al., 2002a). Coagels are hydrated crystalline phases (Capuzzi et al., 1996b; Capuzzi et al., 1997; Palma, 2003; Sapper et al., 1981) and their lamellar structure produces at least one highly ordered dimension (see Fig. 2), so they exhibit sharp X-ray diffraction (XRD) patterns and optical birefringence.

In a coagel, the surfactant hydrocarbon chains have limited freedom of motion, with an interlayer distance of about 10 Å (see Fig. 2). Strongly bound, structured water occupies the space between the surfactant lamellae. The coagel phase is stabilized by interactions between polar head groups, their counterions and solvent molecules. The lipophilic chains are packed in a compact interdigitated order.

CMT for  $ASC_n$  was determined by several techniques such as conductivity and differential scanning calorimetry (DSC). Both of them showed similar values for  $ASC_n$  CMT (Lo Nostro et al., 2003) (see Table 1) which ranged from about 18 °C for  $ASC_8$  to 64 °C for  $ASC_{16}$ . According to Fig. 3, CMT values remain practically constant as the  $ASC_n$  concentration was increased.

On the other hand, at temperature higher than CMT, and depending on the chain length, concentrated dispersions of

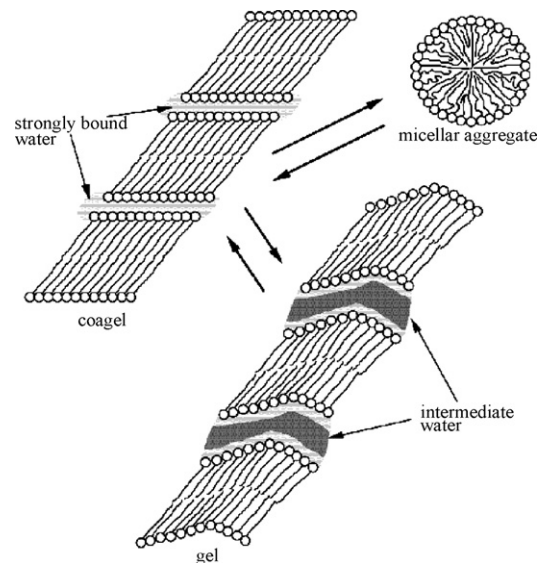


Fig. 2. Schematic picture of a coagel in equilibrium with a micelle or with a gel phase.

surfactants produce either micellar solutions (for  $n \leq 10$ ), or transparent gel phases (for  $n \geq 12$ ) that exhibit a lower degree of crystallinity than coagels. In the gel state, the hydrophobic tails possess a higher degree of freedom, and a temperature increase usually results in an anisotropic expansion of the hydrocarbon chains. This leads to a partial disruption of the packed lamellar structure of the coagel, so that water can penetrate and fill up the gaps between the head groups. Water molecules are present in larger amounts than in the coagel phase; a so-called "intermediate" layer is located between strongly bound layers. Again, the main interactions involve coupling between solvent molecules and the amphiphile headgroups (Lo Nostro et al., 2003). This behavior was confirmed through the evaluation of the effect of other neutral cosolutes such as sucrose and urea (Lo Nostro et al., 2003).

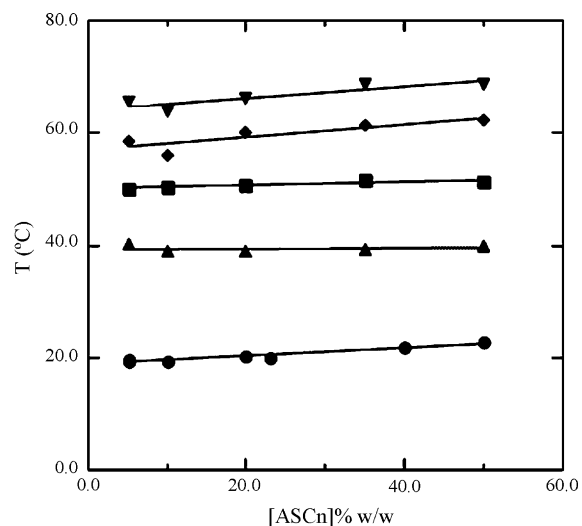


Fig. 3. Phase transition temperature for  $ASC_n$ /water systems as a function of the surfactant concentration, obtained from DSC runs: (●)  $ASC_8$ , (▲)  $ASC_{10}$ , (■)  $ASC_{12}$ , (◆)  $ASC_{14}$ , and (▼)  $ASC_{16}$  (from Lo Nostro et al., 2003).

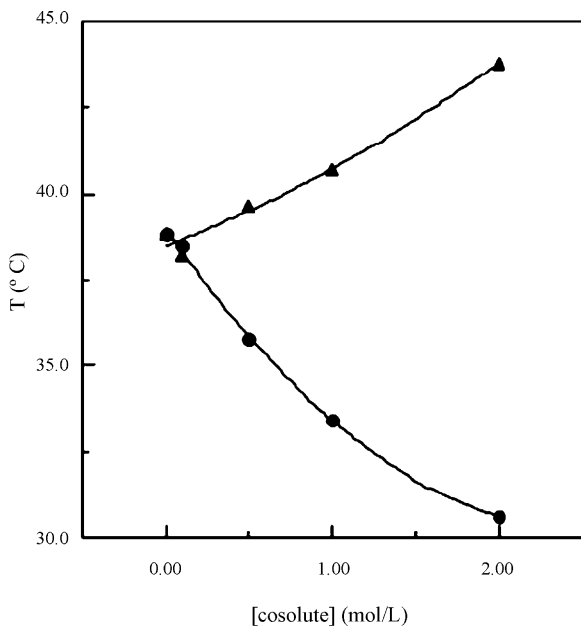


Fig. 4. Effects of sucrose (▲) and of urea (●) on the coagel to micelle transition temperature for a 10% ASC10 sample (from Lo Nostro et al., 2003).

Fig. 4 shows the temperature of the coagel to micelle phase transition as a function of the cosolute concentration. Sucrose leads to a significant increase of the phase transition temperature strengthening the hydrogen bonding network. So, higher temperature is necessary to disrupt the lamellar coagel structure and turn the compact coagel structure into a liquid micellar phase. Instead, urea breaks down the hydrogen bonding network, and the phase transition shifts to lower temperatures.

These investigations confirm that the main factor that dictates the phase behavior of coagels is the interactions between the head groups and the solvent (and with cosolutes if present).

The transition temperature and enthalpy change depend on the length of the aliphatic chain, showing that the conformation and packing of the hydrophobic tails also affect the phase behavior. When the transition temperature (CMT, Fig. 5) and enthalpy change ( $\Delta H$ , Fig. 6) of the phase change are correlated with the melting point of solid pure  $ASC_n$ , a linear relationship between these parameters is observed. This means that the phase change of  $ASC_n$  is mainly ruled by the partial melting of the hydrocarbon side chains.

The kind of assembly produced by a particular surfactant can then be predicted by calculating the *packing parameter*,  $p = v_H/a_0 I_H$  where  $v_H$  is the volume occupied by the hydrophobic chain,  $a_0$  is the area per polar head group, and  $I_H$  is the length of the lipophilic chain in its fully stretched conformation. These values are shown in Table 2. The calculation of  $p$  gives values of about 0.24 and 0.36 for  $ASC_8$  and  $ASC_{10}$ , characteristic and necessary for small, nearly spherical aggregates (Israelachvili et al., 1976; Palma et al., 2002b, 2003a). Macroscopic observations of the phase behavior of  $ASC_n$  in 10% aqueous dispersions indicate that  $ASC_8$  and  $ASC_{10}$  coagels form liquid micellar phases upon heating. In contrast,  $ASC_{11}$ ,  $ASC_{12}$ ,  $ASC_{14}$ , and  $ASC_{16}$  samples show coagel-to-gel phase transitions. They do not form micellar dispersions, at least below 80 °C. The phenomena are

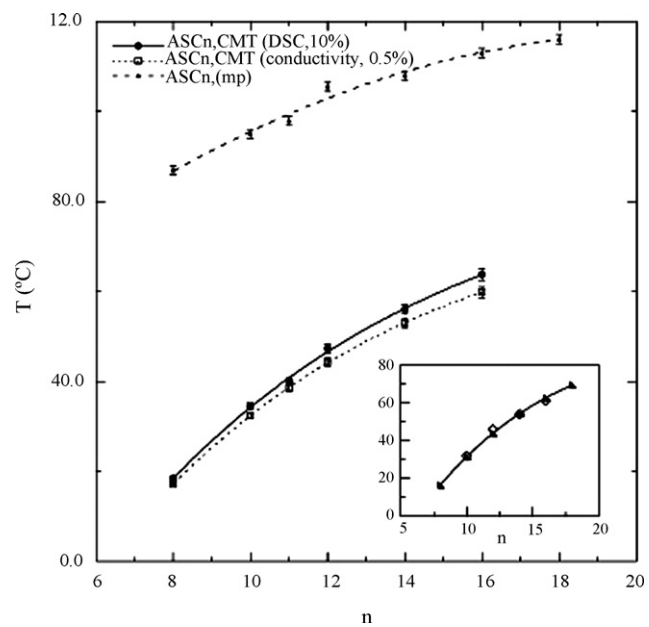


Fig. 5. Relationship between TMC ((○) by DSC, (●) by conductivity) and melting point of: (◊) fatty acids and (▲)  $ASC_n$  (from Palma et al., 2002a).

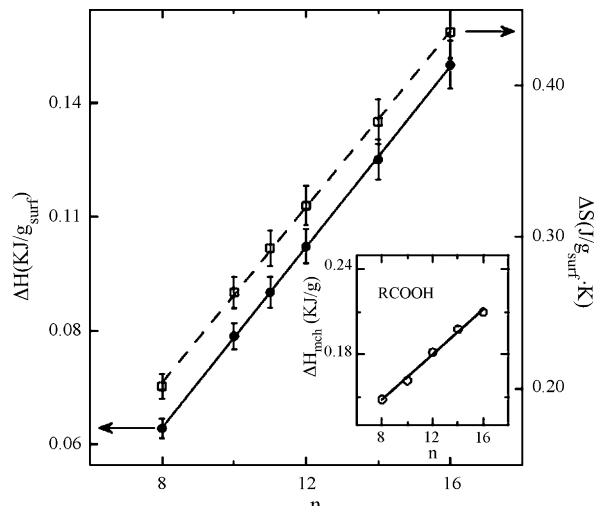


Fig. 6. Enthalpy (in  $kJ/g_{surf}$ , ●) and entropy (in  $J/g_{surf}$ , ○) changes of phase transition obtained from DSC experiments, as a function of the aliphatic tail length (from Palma et al., 2002a).

Table 2

Structural parameters for  $ASC_n$ : volume ( $v_H$ ) and length ( $I_H$ ) of the hydrocarbon chains, cross-section of the polar headgroups ( $a_0$ ) and packing parameter ( $p = v_H/a_0 I_H$ ) (Palma, 2003)

n	$v_H (\text{Å}^3)$	$I_H (\text{Å})$	$a_0 (\text{Å}^2)$	P
8	243	11.6	65	0.24
10	296	14.1	51	0.36
12	350	16.7	37	0.57
14	404	19.2	21	1.04
16	456	21.7	21	1.04

fully reversible to temperature cycles. Similar behavior has been reported for octadecyltrimethylammonium halides (Kodama and Seki, 1991).

Theory shows that for  $1/3 < p < 1/2$ , hexagonal phases are the optimal state preferred if the hydrocarbon chains are truly fluid. As  $p$  increases above  $1/2$  (with increasing chain length) two possibilities occur: if the chains are stiff the system jumps immediately to lamellar (or cubic) phases. If the chains are not rigid, it passes through unilamellar vesicles of increasing size and on to multi-walled vesicles and eventually to lamellar phases as the surfactant parameter increases towards unity. The parameter exceeds  $1/2$  for  $n > 10$  (Table 2), the absence of hexagonal phases and coexistence of gels and coagels with increasing temperature is exactly as one would expect. Optical microscopy (both in transmitted and polarized light) shows the presence of different textures depending on the surfactant and temperature (Fig. 7). ESEM pictures (Fig. 8) confirm the presence in the coagel of a 3-D network of entangled crystalline plates that entrap water. This 3-D network is clearly a consequence of the rapid growth of rigid plates from the gel at the Krafft temperature. X-ray profiles showed differences between coagel and gel phases. X-ray diffractograms (XRD) of anhydrous ASC<sub>14</sub> and its coagel confirm the tight lamellar structure for ASC<sub>n</sub>/water coagels (Figs. 9 and 10) (Ambrosi et al., 2004). Comparing the different patterns for ASC<sub>14</sub>, it is evident that the crystalline structure of the pure anhydrous powder is almost fully maintained in the aqueous mixtures, as the peak (a) at about  $2\theta \approx 2^\circ$  and its higher order reflections show. Furthermore, all profiles show the presence of two relevant peaks (b and c) at about  $8.5^\circ$  and  $12.6^\circ$ , whose intensity depends on the amount of water. The peaks between  $18^\circ$  and  $25^\circ$  reflect the hydrocar-

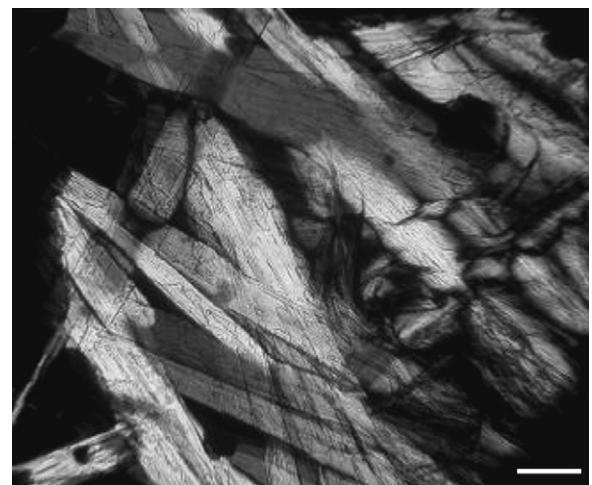
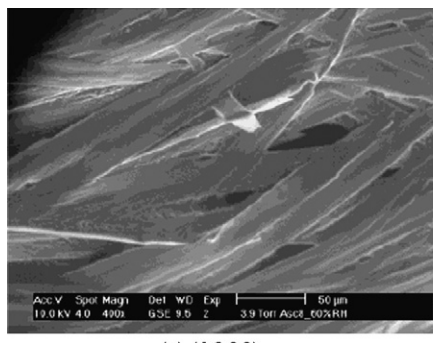


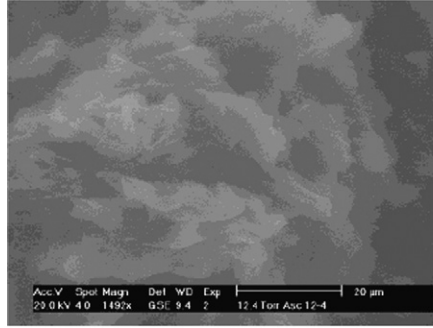
Fig. 7. Optical micrograph of 10% ASC<sub>14</sub>/water coagel; bar = 10  $\mu$ m (from Ambrosi et al., 2004).

bon chain ordering. In particular, the occurrence of peaks for  $20^\circ \leq 2\theta \leq 23^\circ$  indicates either an orthorhombic ( $O_{\perp}$ ) or a monoclinic ( $M_{||}$ ) packing. From Fig. 10 it is clear that peak (a) shifts to lower angles as the hydrophobic chain becomes longer. At 25  $^\circ$ C, ASC<sub>8</sub> produces a quite noisy XRD that shows only the main peak, while the other surfactants produce similar but more structured patterns (Ambrosi et al., 2004).

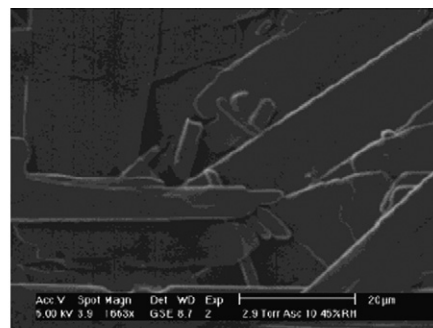
Calorimetric studies showed the presence of two types of water in the coagel phase: (i) bulk, free water that freezes and then melts at about 0  $^\circ$ C, and (ii) frozen, strongly bound water that does not melt in the temperature range investigated. Strongly bounded water molecules form a thin compartment sandwiched



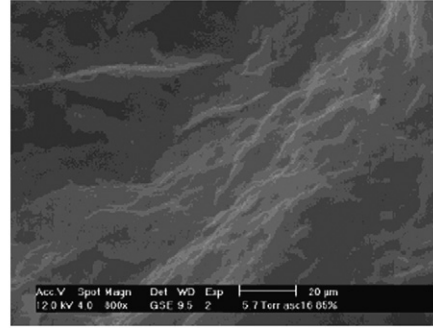
(a) (ASC8)



(c) (ASC12)



(b) (ASC10)



(d) (ASC16)

Fig. 8. ESEM pictures of ASC<sub>n</sub>. (a) ASC<sub>8</sub>, 400x, RH 60%, 3.9 Torr. (b) ASC<sub>10</sub>, 1663x, RH 45%, 2.9 Torr. (c) ASC<sub>12</sub>, RH 70%, 12.4 Torr. (d) ASC<sub>16</sub>, 800x, RH 85%, 5.7 Torr (from Palma et al., 2002a).

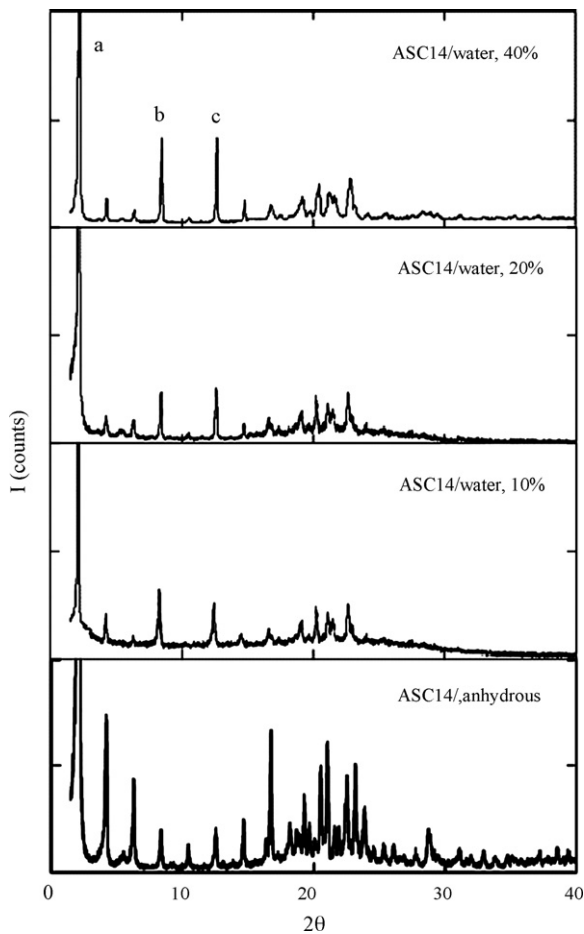


Fig. 9. XRD for anhydrous ASC<sub>14</sub> and its coagels in water at room temperature (from Ambrosi et al., 2004).

between the surfactant bilayers, whereas bulk water surrounds the plate like “islands” and dissolves the few monomers in equilibrium with the coagel phase (Fig. 11) (Ambrosi et al., 2004).

### 3. Aggregates and nanostructures as drug delivery systems

#### 3.1. Drug load capacity

The great hydrophobic environment of the ASC<sub>n</sub> coagels seems to be an interesting tool for the loading of drugs with low aqueous solubility. Furthermore, the use of vitamin C-based surfactants for micellar solubilization is crucial when the hydrophobic solute is particularly sensitive to light, heat, oxidizing materials and radicals, as the ascorbic polar head groups may provide an efficient shield against these degrading agents, and particularly towards dissolved molecular oxygen. ASC<sub>10</sub> supramolecular assemblies dissolve hydrophobic drugs such as danthron, phenacetin and griseofulvin in their lipophilic inner cores, and significantly enhance their solubility and availability in the aqueous phase, with respect to pure water (Palma et al., 2003a).

The incorporation of anthralin, a very unstable drug in solution, has been assayed in ASC<sub>n</sub> coagels. The semisolid

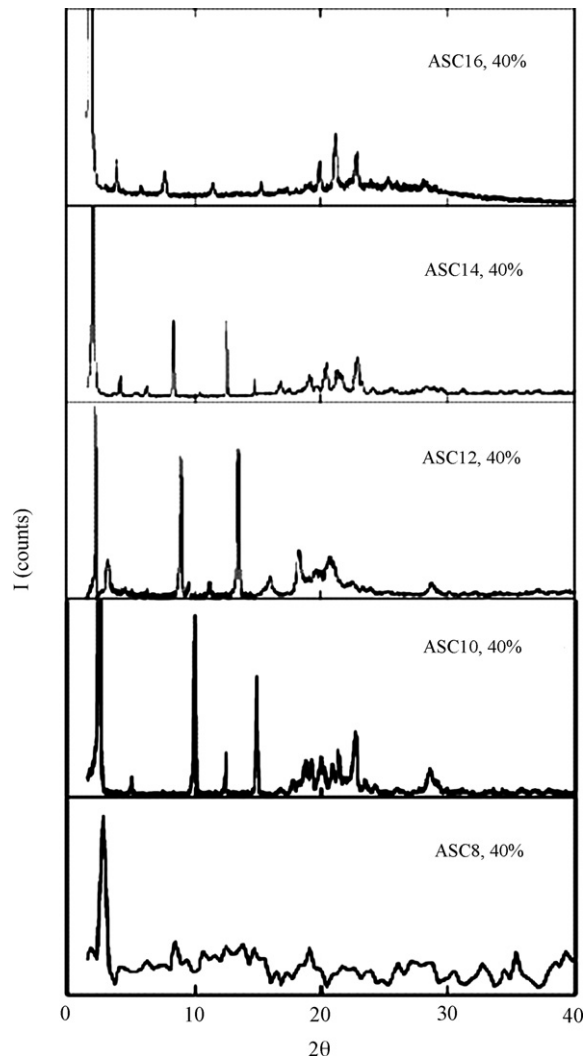


Fig. 10. XRD for ASC<sub>8</sub>, ASC<sub>10</sub>, ASC<sub>12</sub>, ASC<sub>14</sub>, and ASC<sub>16</sub> coagels at 40% and at room temperature (from Ambrosi et al., 2004).

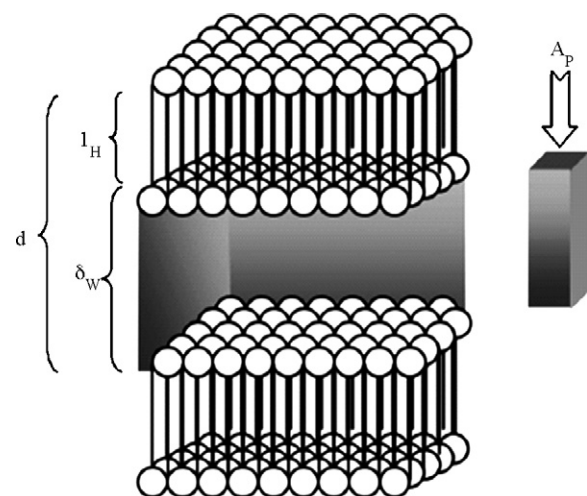


Fig. 11. Schematic picture of the microscopic structural model. The grey area represents the interlayer water. Fully stretched chain length ( $I_H$ ), hydrophilic layer thickness ( $\delta_w$ ), and hydrated headgroup area per amphiphile ( $A_p$ ) (from Ambrosi et al., 2004).

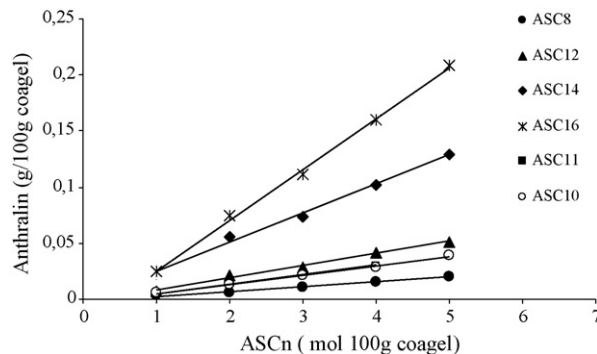


Fig. 12. Solubilization of anthralin in  $ASC_n$  aggregates (from Palma et al., 2003b).

drug loaded system can be obtained through a sequence of heating–cooling cycles of the aqueous suspensions of  $ASC_n$  around the CMT, where the insoluble drug is also dispersed (Palma et al., 2003b). After cooling the drug is located inside of the hydrophobic environment of the lamellae. For all derivatives, an increase in drug solubilization was observed (Fig. 12). The loading capacity of each  $ASC_n$  coagel can be quantitatively related to the slope of the curves from Fig. 12. When these slopes were correlated with the length of the side chain (Fig. 13),

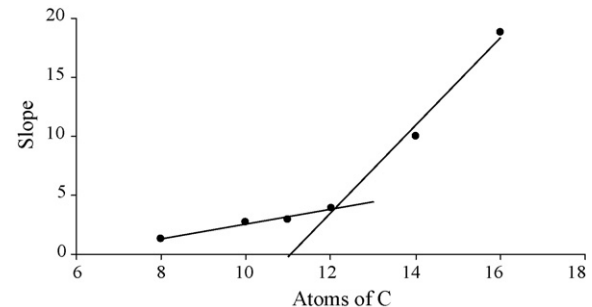


Fig. 13. Relationship between loading capacity and alkyl chain length of  $ASC_n$  (from Palma et al., 2003b).

the loading capacity for  $ASC_n$  with  $n > 12$  shows a very important increase. This observation is in line with the fact  $ASC_{12}$ ,  $ASC_{14}$  and  $ASC_{16}$  form gel structures above CMT, where a large hydrophobic media is available for solubilization. This lamellar configuration is able to incorporate larger drug amounts above CMT, comparative to micellar dispersions formed for  $ASC_8$ ,  $ASC_{10}$  and  $ASC_{11}$  (Palma et al., 2003b). Besides, anthralin solubilized in coagel showed higher stability comparative to ethanolic/aqueous solutions. This drug remains inalterable in  $ASC_{16}$  coagel during at least 4 months, while in ethanolic solu-

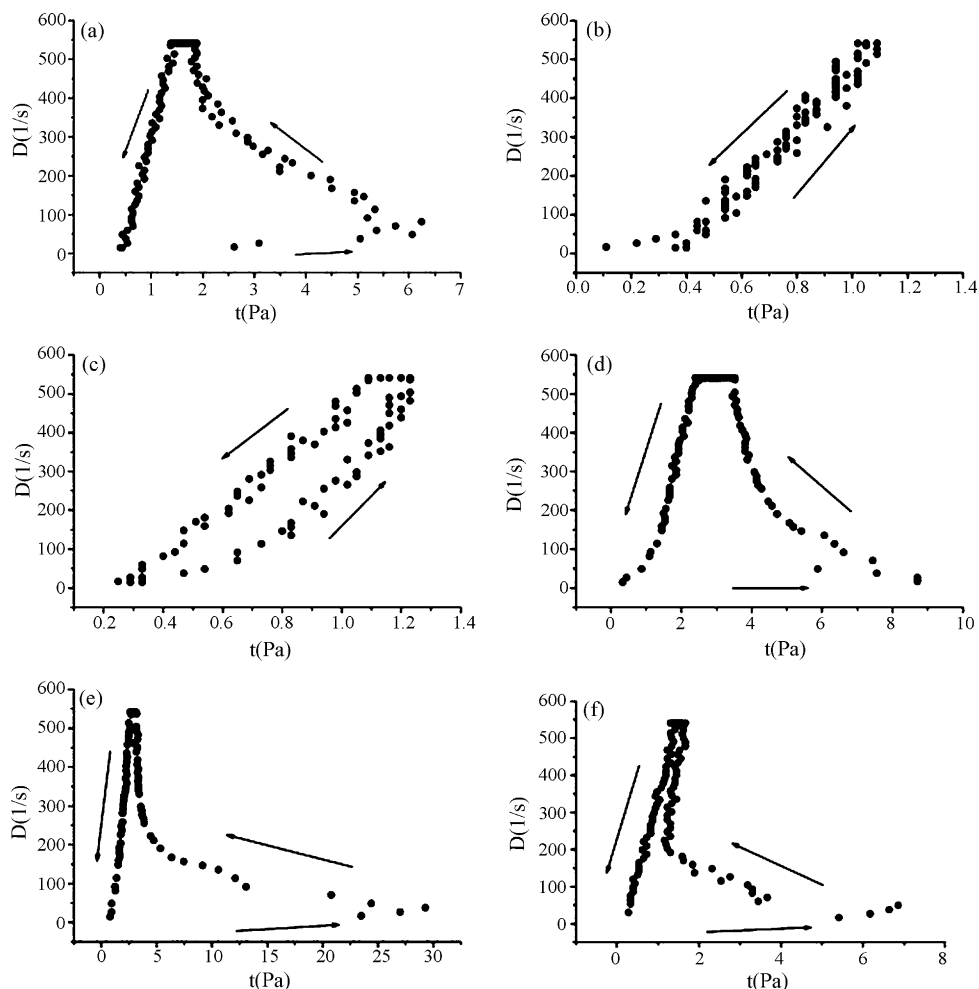


Fig. 14. Rheograms for  $ASC_n$  coagels: (a)  $ASC_8$ ; (b)  $ASC_{10}$ ; (c)  $ASC_{11}$ ; (d)  $ASC_{12}$ ; (e)  $ASC_{14}$ ; and (f)  $ASC_{16}$ .

tion, anthralin concentration decrease to 14.2% in 3 weeks. The addition of  $ASC_{16}$  to the ethanolic solution has negligible effect on the stability of the drug (degradation of 15.9% in 3 weeks) (Palma et al., 2003b). In this way, the hydrophobic interior of the lamellae must be responsible for the protection to oxidative degradation.

The formation of vesicles from  $ASC_{16}$  aggregates has been investigated.  $ASC_{16}$  can form stable vesicles (“aspasomes”) only in presence of cholesterol and negatively charged lipid dicetyl phosphate. The thin film of ascorbyl palmitate on hydration did not form vesicles. Vesicles were seen in all the preparations containing 18–72 mol% of cholesterol; they were spherical and majority of them were multi-lamellar. Very few large unilamellar vesicles were also seen. The antioxidant potency of aspasome was much better than that of ascorbic acid. The encapsulating of zidovudine (AZT) in such vesicular system is reported (Gopinath et al., 2004). The entrapment efficiency of AZT in aspasomes was around 20–30% depending mainly from cholesterol concentration, which also affected the drug release. Significant changes in release were observed with change in cholesterol content in the bilayer of aspasome. Aspasomal AZT showed much slower release rate than AZT solution (Gopinath et al., 2004).

### 3.2. Rheology of nanostructured aggregates

As can be seen in Fig. 14,  $ASC_8$ ,  $ASC_{12}$ ,  $ASC_{14}$ , and  $ASC_{16}$  coagels show a complex rheology, with the appearance of spur rheograms, while coagels of  $ASC_{10}$  and  $ASC_{11}$  exhibit pseudoplastic flow.  $ASC_{11}$  also shows thixotropy. The structural arrangement of these systems is the main factor that accounts for this behavior. Coagels of  $ASC_{12}$ ,  $ASC_{14}$  and  $ASC_{16}$  form a ‘house of cards’ structure, where swelling and strengthening of the semisolid network occurs, due to the presence of water pools between the amphiphilic bilayers. On the other hand, for  $ASC_{10}$  and  $ASC_{11}$  coagels, this kind of arrangement apparently is not permitted and flexible bimolecular sheets arrange parallel to each other. A characteristic feature of many such rheograms is the presence of a ‘spur’ point on the ascending curve. Rheologies of these coagels display a high yield or spur value and the shear stress at spur point is called the ‘static yield value’ ( $\sigma_S$ ). This can be taken as a measure of the strength and for such systems an irreversible structure breakdown is observed when the shear stress exceeds  $\sigma_S$ . The original coagel structure is not restored on rest. The values observed for  $\sigma_S$  are proportional to the alkyl chain length for  $ASC_8$ ,  $ASC_{12}$  and  $ASC_{14}$ . The relatively low value for  $ASC_{16}$  coagel indicates a less structured network. When the spur value is reached, the secondary structure of coagels is broken and  $ASC_{12}$ ,  $ASC_{14}$  and  $ASC_{16}$  coagels acquire pseudoplastic flow (Palma et al., 2003c).

### 3.3. “In vitro” permeation of $ASC_n$ and influence in drug absorption (enhancement properties)

The permeation of  $ASC_n$  as well as its effect on “in vitro” and “in vivo” drug diffusion through rat skin was evaluated (Palma

et al., 2006). Penetration of  $ASC_n$  through rat skin epidermis was very fast and quantitatively significant.  $ASC_{12}$  appears to be the compound that possesses the highest capacity to enhance the penetration of the drug as well as for self-penetration through the epidermis. The ability of these compounds to permeate the rat skin is related to their chemical composition, since the flux of  $ASC_n$  decreases as alkyl chain length increases. Furthermore, a burst effect was observed with  $ASC_{12}$ .

$ASC_n$  coagels containing FITC (fluorescein isothiocyanate, hydrophobic fluorescent marker) were put in contact with the dorsal sides of mice ears. Fluorescent microscopy showed that  $ASC_{16}$  coagel exhibited a thin external fluorescent line. With  $ASC_{14}$  the marker was only observed in the stratum corneum (SC), while for  $ASC_{12}$  the fluorescence was detected in the whole epidermis (Fig. 15a and b, respectively). In all cases the fluorescent marker was not visualized in the dermis. These results indicate that  $ASC_{12}$  seems to have the highest enhancing effect on FITC permeation. Also, the permeation of anthralin from  $ASC_n$  coagels applied on rat skin was very increased (Palma et al., 2006) compared to other pharmaceutical systems such as liposomal and niosomal carriers (Agarwal et al., 2001), being  $ASC_{12}$  the most effective enhancer. This is in coincidence with the observed for FITC. Absence of side effects in the epidermis after the application of  $ASC_n$  coagels was observed.

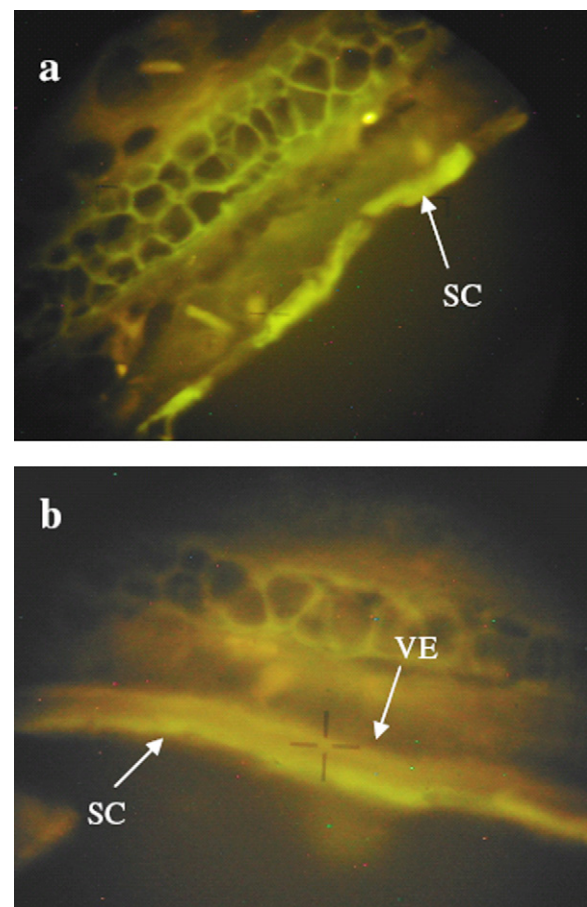


Fig. 15. Fluorescent microscopy of  $ASC_n$  coagels containing FITC. (a)  $ASC_{14}$ , (b)  $ASC_{12}$  (SC, stratum corneum; VE, viable epidermis).

#### 4. Summary and perspective

The attachment of *n*-alkyl fatty chain at position 6 of VC permits to obtain a series of derivatives with two main particular properties. By one side, the lipophilic character is significantly increased and, by the other, surfactant properties are added to the new compounds. Like so,  $ASC_n$  have self-assembly properties forming different aggregates.  $ASC_n$  assemblies are able to solubilize drugs at temperatures in which the solubility reaches the CMC (CMT). Above this temperature,  $ASC_n$  can aggregate in micelles or gel phase, depending of alkyl side chain. Upon cooling, for less soluble derivatives ( $ASC_{12}$ ,  $ASC_{14}$  and  $ASC_{16}$ ) liquid-crystal structures called coagels are obtained. These systems possess very interesting properties that make  $ASC_n$  coagel a promising pharmaceutical platform for drug delivery. They are able to solubilize insoluble and unstable drugs, protect them from any possible aggressive environment and promote their permeation through skin. Besides, the rheological properties of the coagels would be adequate for topical administration. In conclusion,  $ASC_n$  coagels present great possibilities for pharmaceutical formulation with potential administration of drugs by different routes of administration.

#### Acknowledgements

Partial financial support from Consejo Nacional de Investigaciones Científicas y Técnicas (CONICET), FONCyT Préstamo BID 1278/OC-AR, Proy. No. 05–10954 and SECyT-UNC, is greatly acknowledged.

#### References

Agarwal, R., Katare, O., Vyas, S., 2001. Preparation and in vitro evaluation of liposomal/niosomal delivery systems for antipsoriatic drug dithranol. *Int. J. Pharm.* 228, 43.

Ambrosi, M., Lo Nostro, P., Fratoni, L., Dei, L., Ninham, B.W., Palma, S., Manzo, R., Allemandi, D., Baglioni, P., 2004. Water of hydration in coagels. *Phys. Chem. Chem. Phys.* 6, 1401.

Ambrosi, M., Fratini, E., Alfredsson, V., Ninham, B.W., Giorgi, R., Lo Nostro, P., Baglioni, P., 2006. Nanotubes from a vitamin C-based bolaamphiphile. *J. Am. Chem. Soc.* 128, 7209.

Capuzzi, G., Lo Nostro, P., Kulkarni, K., Fernandez, J., Vincieri, F., 1996b. Interactions of 6-*O*-stearoylascorbic acid and vitamin K1 in mixed Langmuir films at the gas–water interface. *Langmuir* 12, 5413.

Capuzzi, G., Lo Nostro, P., Kulkarni, K., Fernandez, J., 1996a. Mixtures of stearoyl-6-*O*-ascorbic acid and -tocopherol: a monolayer study at the gas/water interface. *Langmuir* 12, 3957.

Capuzzi, G., Kulkarni, G., Fernandez, J., Vincieri, J., Lo Nostro, P., 1997. Mixture of ascorbyl-steareate and vitamin D3: a monolayer study at the gas–water interface. *J. Colloid Interface Sci.* 186, 271.

Clint, J., 1992. Surfactant Aggregation. Blackie, London.

Djerassi, D., 1997. The role of the corrective vitamins A, B5 and C in the new, high performance cosmetics. *Drug Cosmet. Ind.* 160, 60.

Gopinath, D., Ravi, D., Rao, B., Apte, S., Renuka, D., Rambhau, D., 2004. Ascorbyl palmitate vesicles (Aspasomes): formation, characterization and applications. *Int. J. Pharm.* 271, 95.

Israelachvili, J., Mitchell, D., Ninham, B.W., 1976. Theory of self-assembly of hydrocarbon amphiphiles into micelles and bilayers. *J. Chem. Soc., Faraday Trans.* 72, 1525.

Kleszczewska, E., 2000. L-Ascorbic acid—clinical use, toxicity, properties, methods of determination and application in chemical analysis. *Pharmazie* 55, 640.

Kodama, M., Seki, S., 1991. Thermodynamical investigations on phase transitions of surfactant–water systems: thermodynamic stability of coagel and coagel phases and the role of water molecules in the appearance. *Adv. Colloid Interface Sci.* 35, 1.

Kohler, U., Yang, P., Weng, S., Mantsch, H., 1988. *Can. J. Spectrosc.* 33, 122.

Lo Nostro, P., Ramsch, R., Fratini, E., Lagi, M., Ridi, F., Garretti, E., Ambrosi, M., Ninham, B.W., Baglioni, P., 2007. Organogels from a vitamin C-based surfactant. *J. Phys. Chem. B* 111, 11714–11721, doi:10.1021/jp0730085.

Lo Nostro, P., Capuzzi, G., Mulinacci, N., 2000a. Self-assembly and antioxidant properties of octanoyl-6-*O*-ascorbic acid. *Langmuir* 16, 1744.

Lo Nostro, P., Capuzzi, G., Pinelli, P., Mulinacci, N., Romani, A., Vincieri, F., 2000b. Self-assembling and antioxidant activity of some vitamin C derivatives. *Colloids Surf. A: Physicochem. Eng. Aspects* 167, 83.

Lo Nostro, P., Ninham, B., Fratoni, L., Palma, S., Manzo, R., Allemandi, D., Baglioni, P., 2003. Effect of water structure on the formation of coagels from ascorbyl-alkanoates. *Langmuir* 19, 3222.

Myers, D., 1994. Surfactant Science and Technology, second ed. VCH, New York, p. 83.

Palma, S., 2003. Estudio de compuestos anfífilicos y su utilización en tecnología farmacéutica. PhD Thesis. Universidad Nacional de Córdoba, Córdoba, Argentina.

Palma, S., Manzo, R., Allemandi, D., Fratoni, L., Lo Nostro, P., 2003a. Drugs solubilization in ascorbyl-decanoate micellar solutions. *Colloids Surf. A: Physicochem. Eng. Aspects* 212, 163.

Palma, S., Manzo, R., Lo Nostro, P., Fratoni, L., Allemandi, D., 2003b. Vehiculización de Antralina en coageles de *n*-alquil derivados del Ácido Ascórbico. S. Palma, R. Manzo, P. Lo Nostro, L. Fratoni y D. Allemandi. Acta Farmacéutica Bonaerense 22, 305.

Palma, S., Jiménez-Kairuz, A., Fratoni, L., Lo Nostro, P., Manzo, R., Allemandi, D., 2003c. Coagels from 6-*O*-alkyl ascorbic acid derivatives as drug carriers: structure and rheology. *II Farmaco* 58, 1271.

Palma, S., Maletto, B., Lo Nostro, P., Manzo, R., Pistoresi-Palencia, M., Allemandi, D., 2006. Potential use of ascorbic acid based surfactants as skin penetration enhancers. *Drug Dev. Ind. Pharm.* 32, 1.

Palma, S., Manzo, R., Allemandi, D., Fratoni, L., Lo Nostro, P., 2002a. Coagels from ascorbic acid derivatives. *Langmuir* 18, 9219.

Palma, S., Manzo, R., Allemandi, D., Fratoni, L., Lo Nostro, P., 2002b. Solubilization of hydrophobic drugs in octanoyl-6-*O*-ascorbic acid micellar dispersions. *J. Pharm. Sci.* 91, 1810.

Rowe, R.C., Sheskey, P.J., Owen, S.C., 2006. Handbook of Pharmaceutical Excipients, fifth ed. Pharmaceutical Press, London.

Sapper, H., Cameron, D., Mantsch, H., 1981. The thermotropic phase behavior of ascorbyl palmitate: an infrared spectroscopic study. *Can. J. Chem.* 59, 2543.

Shibayama, H., Ueda, K., Yoshio, K., Matsuda, S., Hisama, M., Miyasawa, M., 2005. Synthesis and characterization of new ascorbic derivative: sodium isostearyl 2-*O*-L-ascorbyl phosphate. *J. Oleo Sci.* 54, 601–608.

Silva, G.M., Maia Campos, P.M., 2000. Ascorbic acid and its derivatives in cosmetic formulations. *Cosmet. Toil* 115, 59.